Pergamon

Cement and Concrete Research 33 (2003) 325–332

CEMENT AND CONCRETE RESEARCH

Effects of gypsum formation on the performance of cement mortars during external sulfate attack

Manu Santhanam[a], Menashi D. Cohen[b,*], Jan Olek[b]

[a]*Department of Civil Engineering, IIT Madras, Chennai 600036, India*
[b]*School of Civil Engineering, Purdue University, West Lafayette, IN 47907, USA*

Received 18 April 2001; accepted 31 July 2002

Abstract

Sodium sulfate attack was studied on C_3S mortars, along with ASTM Type I Portland cement (PC) mortars, in an attempt to independently evaluate the effect of gypsum formation on the performance. The quantity of gypsum and ettringite, as measured by differential scanning calorimetry (DSC), increased with the time of immersion in the sulfate solution. An increase in length of the mortar specimens was also registered along with the increase in the quantity of gypsum. This result suggests that the formation of gypsum could be expansive. Indeed, considerable expansion, although delayed compared to PC mortars, was observed in the C_3S mortars. Thus, it can be concluded that the expansion of the PC mortars occurred due to the combined effect of gypsum and ettringite formation, while the expansion of C_3S mortars occurred as a result of gypsum formation. Thaumasite formation as small inclusions was also detected in both the C_3S and the PC mortars, especially in regions of high gypsum deposition. The formation of thaumasite, despite the absence of carbonate bearing minerals and low temperatures, could be because of the carbonation of the surface zones of the mortars. However, it would be speculative to attribute any expansion to the formation of thaumasite, since it was detected only in minute amounts in the microstructural investigation.

Keywords: Sulfate; Ettringite; Expansion; Thermal analysis; Thaumasite

1. Background

Sulfate attack has been traditionally studied from the perspective of ettringite formation. Low C_3A cements were developed to combat sulfate-related damage by minimizing the formation of ettringite, which is known to cause expansion when present in excessive amounts. However, in field studies, the evidence of sulfate attack damage has mostly been spalling and softening of concrete rather than expansion. Laboratory studies, aimed at accelerating sulfate attack using solutions of high sulfate concentration, also show distress in the form of spalling and softening of concrete, in addition to cracking resulting from expansion. In these accelerated tests, gypsum formation has been recognized as one of the principal causes of damage. The exact nature of disruption caused by gypsum, however, is not well established. Softening of the concrete surface, rather than expansion, has been attributed to the effect of gypsum. Theories have been proposed, some supporting and others opposing the possibility that gypsum can cause expansion. This article reports on the physical, chemical and microstructural alterations of cementitious mortars brought about by the formation of gypsum during sulfate attack.

The article also discusses another important by-product of sulfate attack—thaumasite—that has been generally ignored in sulfate attack studies. Thaumasite causes a complete break-up of the structure of concrete because it is formed as a result of a direct attack of the C–S–H by the sulfate ions. Thaumasite is believed to form during sulfate attack at low temperatures (0–5 °C) in the presence of CO_3^{2-} or CO_2. Recent evidence, however, has shown that thaumasite can form at higher temperatures.

1.1. Gypsum formation

Gypsum is formed during sulfate attack as a result of the reaction (Eq. (1)) between calcium hydroxide (CH), which is formed during cement hydration, and sulfate ions in

* Corresponding author. Tel.: +1-765-494-5018; fax: +1-765-494-1364.
E-mail address: mcohen@ecn.purdue.edu (M.D. Cohen).

0008-8846/02/$ – see front matter © 2002 Elsevier Science Ltd. All rights reserved.
PII: S0008-8846(02)00955-9

aqueous solutions. The sulfate ions are usually transported to the concrete by groundwater contaminated by Na_2SO_4, $MgSO_4$, $FeSO_4$, $CaSO_4$, etc. The quantity of gypsum produced during the reaction varies with the type or source of the sulfate dissolved in the solution.

$$Ca(OH)_2 + SO_4^{2-} + 2H_2O \rightarrow CaSO_4 \cdot 2H_2O(\text{gypsum}) + 2OH^- \quad (1)$$

In concrete that is damaged by sulfate attack, gypsum is primarily detected close to the surface, especially in cracks and in voids [1]. Gypsum could also form as a layer at or near the surface, when the attacking solution is magnesium sulfate [2]. In the case of magnesium sulfate attack, gypsum formation in bands interspersed with noncementitious magnesium silicate hydrate (MSH) has also been well documented [2].

The effect of gypsum formation on expansion and mechanical degradation is difficult to quantify exactly because it is masked by the formation of ettringite during sulfate attack. Researchers have often attempted to isolate this effect by studying C_3A-free systems. Mehta et al. [3] investigated the performance of concrete specimens prepared with C_3S cement. Long-term exposure was seen to cause spalling and drop in strength of C_3S concrete as compared to concrete prisms prepared with ASTM Type V cement. This phenomenon was attributed to gypsum formation, which was confirmed by X-ray diffraction (XRD).

In a study by Tian and Cohen [4], the effect of gypsum formation during sulfate attack on the resulting expansion of C_3S paste and mortar prisms was investigated. The quantity of gypsum formed in various mixtures was compared by the relative heights of the corresponding XRD peaks. C_3S mortars were highly susceptible to expansion and registered a high degree of gypsum formation. Expansion was lower when C_3S was partially substituted by silica fume.

Numerous theories have been suggested both supporting and opposing the possibility that expansion can occur as a result of gypsum formation [4]. According to Hansen [5] and Mather [6], the formation of gypsum according to Eq. (1) would not cause an increase in volume if the reaction proceeds by a through-solution mechanism. In other words, the gypsum that forms as a result of this reaction would not occupy a volume larger than that of the cavity in which it is precipitated plus the solid CH that is dissolved to participate in the reaction. On the other hand, a change in the crystal structure from the reactants to product could cause the inclusion of air voids, as is the case when gypsum forms from hemihydrate [7]. The air void inclusions could result in expansion. Crystal growth pressure and hydraulic pressure have also been suggested as a possible cause of the observed expansion [8].

Thus, it is evident that further studies are necessary to understand the mechanism of damage associated with gypsum formation. At high concentration (>5000 ppm SO_3), the sulfate attack process is driven by the formation of gypsum [9]. Recognizing the effect of gypsum can enable the determination of appropriate cost-effective solutions. For example, admixtures such as sodium citrate may modify the crystal growth habit of gypsum. In the presence of sodium citrate, gypsum deposits in a short and stubby form rather than the normal needle-like form [7]. The use of such materials could reduce the damaging effects of gypsum.

1.2. Thaumasite formation

The formation of thaumasite during sulfate attack on concrete has been reported by researchers [10,11]. Thaumasite is believed to form during sulfate attack at low temperatures (0–5 °C) in the presence of CO_3^{2-} (which could be in the form of dissolved salts or from carbonate aggregates) or dissolved atmospheric CO_2. The nature of the crystal structure of thaumasite is still a subject of controversy with respect to the coordination number of the Si in thaumasite [10]. However, the general reaction for the formation of thaumasite may be summarized by Eq. (2).

$$3CaO \cdot 2SiO_2 \cdot 3H_2O + 2\{CaSO_4 \cdot 2H_2O\} + CaCO_3 + CO_2 + 23H_2O \rightarrow 2Ca_3[Si(OH)_6](CO_3)(SO_4) \cdot 12H_2O \quad (2)$$

According to Eq. (2), thaumasite formation directly involves C–S–H gel, along with a sulfate source and a carbonate source. In an abbreviated form, thaumasite can be written as $CaCO_3{\cdot}CaSO_4{\cdot}CaSiO_3{\cdot}15H_2O$.

The formation of thaumasite during sulfate attack is especially deleterious because the C–S–H is directly involved in this reaction. In other instances, thaumasite has been reported to form as a result of the interaction of ettringite with the C–S–H in the presence of CO_2. In such cases, thaumasite is often found to be in solid solution with ettringite [12]. When the attacking solution includes magnesium sulfate, the formation of thaumasite is accompanied by the formation of secondary gypsum and brucite [11].

A controversy exists regarding the temperature required for thaumasite formation. Although initially it was believed that temperatures below 5 °C were essential for the reaction, evidence of thaumasite formation from sulfate attack investigations in some parts of California having warm climates [1] has shown that the low temperatures need not be essential.

Thaumasite is often indistinguishable from ettringite due to their nearly identical XRD patterns [13]. While ettringite formation is accompanied by expansion and spalling, thaumasite formation has a more severe damaging effect. Thaumasite is able to transform hardened concrete and mortar into a soft pulpy mass because of a direct attack on the C–S–H.

Thaumasite formation and its effect on mortar performance have not been studied in detail. One possible reason for this may be that the formation of thaumasite was not

Table 1
Properties of materials used in the study

	C_3S (%)	C_3A (%)	SO_3 (%)	Alkali (%)	Fineness (cm^2/g)
PC	62.00	9.00	2.67	0.50	3600
C_3S	98.90	Minor	–	–	4000

anticipated at normal testing temperatures (20–35 °C), and discrepancies in experimental observations were overlooked. Now that there is some convincing evidence of thaumasite formation at normal temperatures, it is essential to understand the circumstances related to this effect.

The study reported in this article was primarily conducted to gauge the effect of gypsum formation on the measured physical properties of mortars. The detection of thaumasite in the microanalysis added to the scope of this study.

2. Experimental methods and materials

Some properties and major constituents of the ASTM Type I Portland cement (PC) and the C_3S (monoclinic) used in the study are presented in Table 1. ASTM C778 graded sand was used in the study.

Prismatic specimens having dimensions of $5 \times 16 \times 80$ mm were used to measure expansion, while $4 \times 14 \times 60$ mm prisms were used to obtain specimens for quantitative analysis by differential scanning calorimetry (DSC). Mass change was measured on cylindrical specimens 23 mm in diameter and 80 mm high. The specimens for scanning electron microscopy (SEM) were obtained both from the $4 \times 14 \times 60$ prisms and the 23×80 mm cylinders.

The mortar proportions were 0.485 (water):1.0 (cementitious material):2.75 (sand) by mass. After casting, the specimens were stored in a container inside a 100% RH moist room. The specimens were removed from molds two days after mixing and casting. Subsequently, the specimens were stored in limewater for a period of 12 days. After this common initial curing regime, specimens were stored in two different solutions: a saturated limewater solution (control) and a 4.44 mass % sodium sulfate solution with an equivalent SO_3 of 25 000 ppm (in other words, a SO_4^{2-} concentration of 30 000 ppm and Na^+ concentration of 14 380 ppm). Expansion and mass change of specimens were monitored periodically, along with thermal analysis of companion samples by DSC.

The mortar specimens used for DSC measurements were stored in acetone, for at least 1 day, immediately after removal from the solutions. After removal from acetone, the specimens were ground to a fine powder using a mortar and pestle and passed through a #200 (75 μm opening) sieve. The sand fraction of the mortar was effectively removed in this process. Thus, the material passing the sieve essentially consisted of the paste fraction of the mortar. This material was stored in airtight plastic containers, to be used for DSC experiments within a week from preparation. DSC was conducted at a heating rate of 10 °C/min up to a maximum of 500 °C.

Specimens were prepared for examination in the backscatter electron mode under the SEM. The specimens used for SEM were dried at 70 °C in an oven for 1 day and then embedded in a low-modulus epoxy. The specimens were then polished using progressively smaller grids and coated with a gold-palladium coating. The prepared specimens were stored in vacuum at room temperature.

3. Results

3.1. Expansion measurements

Fig. 1 presents the expansion data for the C_3S and PC mortars stored in the limewater and sodium sulfate solutions. The PC mortars stored in sodium sulfate solution showed a high degree of expansion between the 6th and 12th week of exposure. Complete disintegration of the specimens occurred after about 16 weeks of immersion. The final measured expansion for the PC mortar specimens was 1.02% after 12 weeks of immersion. The C_3S mortars in sodium sulfate

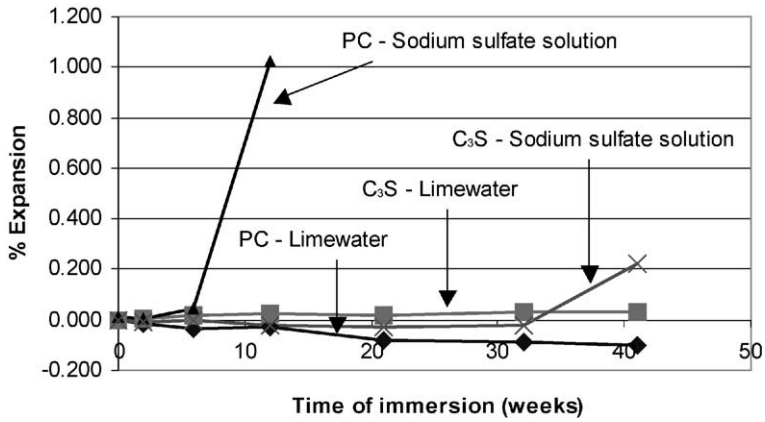

Fig. 1. Expansion data for PC and C_3S mortars.

solution showed small length change during the first 32 weeks of immersion. After 32 weeks, an increase in the rate of expansion was observed. After 41 weeks of immersion, the expansion recorded for the C_3S mortar specimens was 0.22%.

3.2. Mass change measurements

Fig. 2 illustrates the mass change data for the C_3S and PC mortar specimens immersed in the limewater and sodium sulfate solutions. Both PC and C_3S mortars show a steady rate of mass gain when exposed to sodium sulfate solution. The rate of mass increase for C_3S mortar specimens goes up between 21 and 41 weeks of immersion. As per Fig. 1, the expansion also increases dramatically between 32 and 41 weeks of exposure. The PC mortar specimens in limewater show a mass gain of 1%. This could have resulted from the absorption of the limewater by the mortar.

3.3. Thermal analysis by DSC

Fig. 3 shows the results from DSC measurements on the samples of C_3S and PC mortars stored in sodium sulfate solution. The data plotted represent the percentage of the compound (ettringite, gypsum or CH) in the paste fraction of the mortar. The dehydration peaks for ettringite and gypsum occur between 80–100 and 110–135 °C, respectively. The peak for pure thaumasite occurs between 100 and 120 °C. Thus, the presence of thaumasite can lead to marginal errors in the calculation of peak areas for ettringite and gypsum. Also, the stoichiometry of ettringite can also affect its peak position and the total enthalpy of dehydration.

The PC mortars exhibit a steady increase in the amount of ettringite with the duration of immersion. The quantity of gypsum increases substantially from 0.6% at 6 weeks to over 2% at 12 weeks, and then remains constant for the PC mortars. The C_3S mortars show a steady increase in the quantity of gypsum. The quantity of gypsum formed reached 2% between 6 and 12 weeks of immersion for the PC mortars, and between 32 and 41 weeks for the C_3S mortars. This phenomenon is matched by an increase in

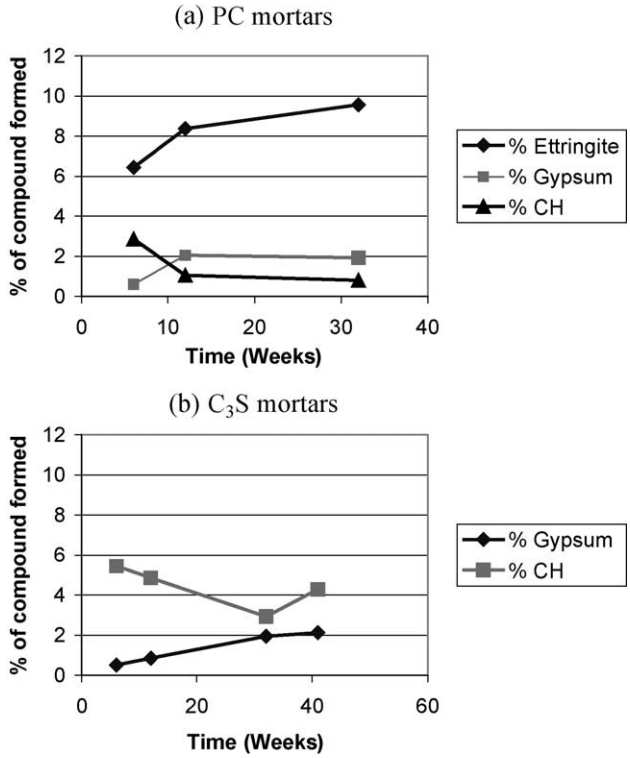

Fig. 3. Results from DSC measurements for specimens stored in sodium sulfate solution.

the expansion, which in the case of the PC mortar is significant (increases from 0.05% to 1.02%), as is evident from Fig. 1. The quantity of CH decreases steadily for both mortars, which is expected as a result of the gypsum-forming reaction (Eq. (1)). The trend of increase in gypsum content is matched by the trend in the reduction of CH content.

3.4. Microstructural studies by SEM

The micrographs presented in this section are divided into three parts: (1) the top left corner shows a low

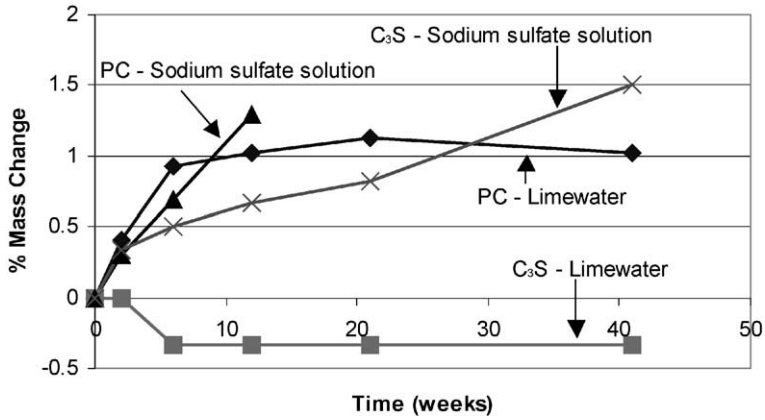

Fig. 2. Mass change data for PC and C_3S mortars.

magnification view of the mortar, (2) a magnified area from the low magnification view (highlighted by a white square) is presented in the top right corner and (3) the bottom portion of the micrograph presents the X-ray spectrum collected for the area highlighted by a box on the top right image.

A micrograph of PC mortar cured in limewater solution is presented in Fig. 4. Decalcified C–S–H can be observed near the surface, as shown by the darker paste near the surface on the right-hand image, and the corresponding X-ray spectrum. The decalcification could have resulted possibly from the paste getting washed out by the surrounding solution. A layer of calcite is also visible at the surface. This could have formed due to some carbonation when the specimen was removed from solution. The paste in the interior showed normal features, such as deposits of CH around aggregates and C–S–H with normal C/S ratios ($\sim$1.7). Fig. 5 shows the micrograph of a C_3S mortar cured in limewater solution. The C_3S mortar specimen appears to have suffered a higher degree of wash out from the surrounding solution, as evident from the low magnification image (on the left), showing the porous zone extending almost 1 mm into the specimen.

The microstructural appearance of PC mortar immersed in sodium sulfate solution changes with the duration of immersion. Figs. 6 and 7 show the microstructure of the PC mortar after 12 weeks of immersion. In Fig. 6, a deposit of monosulfate under a surface layer of calcite can be observed. Such monosulfate deposits were also seen in the interior of the specimen. The C–S–H gel present in the near surface region had a smeared out texture and was found to be decalcified. Fig. 7 shows an air void near the surface of the mortar, with a deposit of gypsum lining the void. The C–S–H surrounding this deposit appears highly cracked and contains small inclusions, which were determined to be a mixture (or a solid solution) of thaumasite and ettringite by energy dispersive X-ray analysis.

Figs. 8–11 show the micrographs for the PC mortar specimens immersed in sodium sulfate solution for 32 weeks. The PC mortar specimen appears highly disintegrated with a network of interconnected cracks. This is evident from the

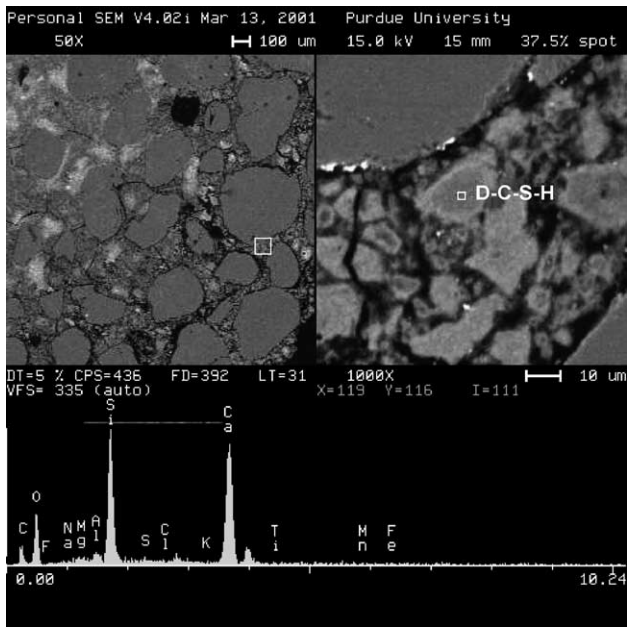

Fig. 5. C_3S mortar stored in limewater showing a washed out surface zone and reduced C/S ratios for the C–S–H in the surface zone.

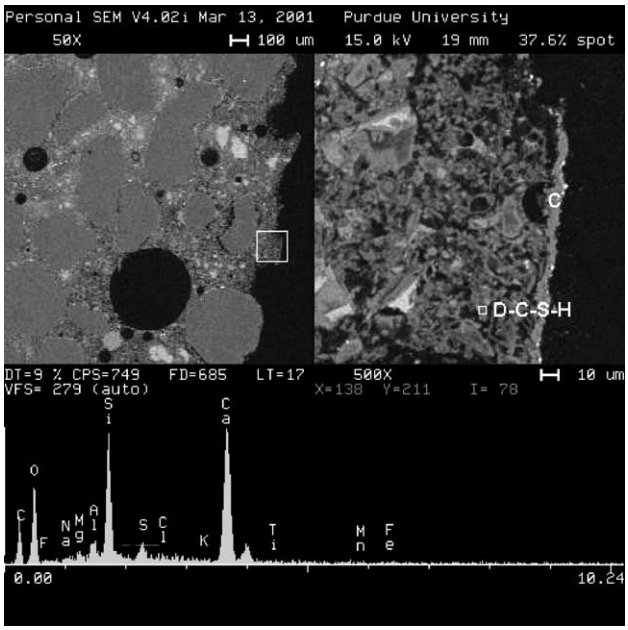

Fig. 4. PC mortar specimen in limewater showing the formation of a calcite layer at the surface and a porous paste with decalcified C–S–H gel (D–C–S–H) just under the surface.

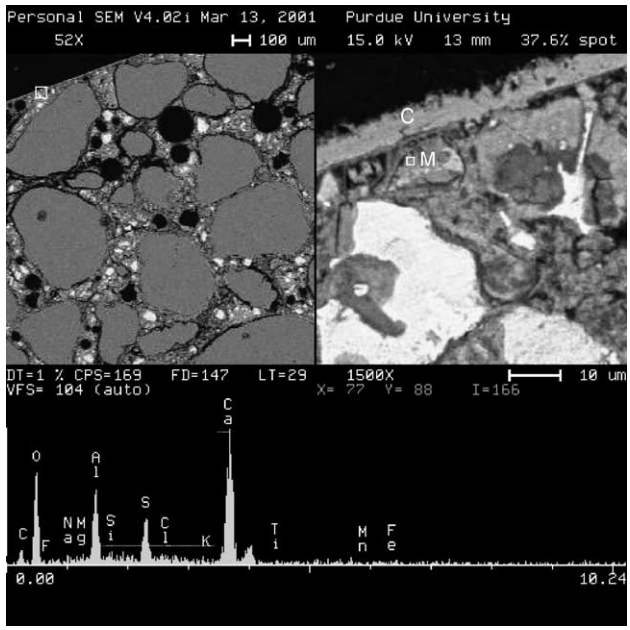

Fig. 6. PC mortar stored for 12 weeks in Na_2SO_4 solution, showing a calcite layer (C) at the surface and a monosulfate deposit (M) just under the surface.

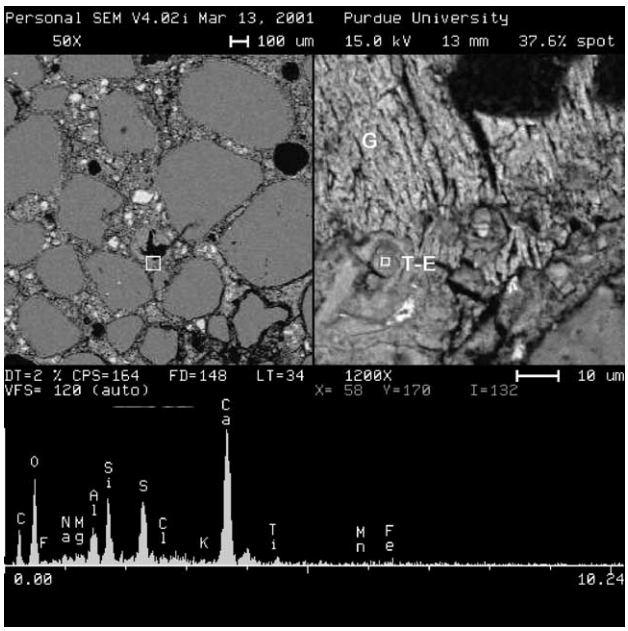

Fig. 7. PC mortar stored for 12 weeks in Na_2SO_4 solution, showing extensive deposition of gypsum (G), along with a possible deposit of a mixture of ettringite and thaumasite (T–E).

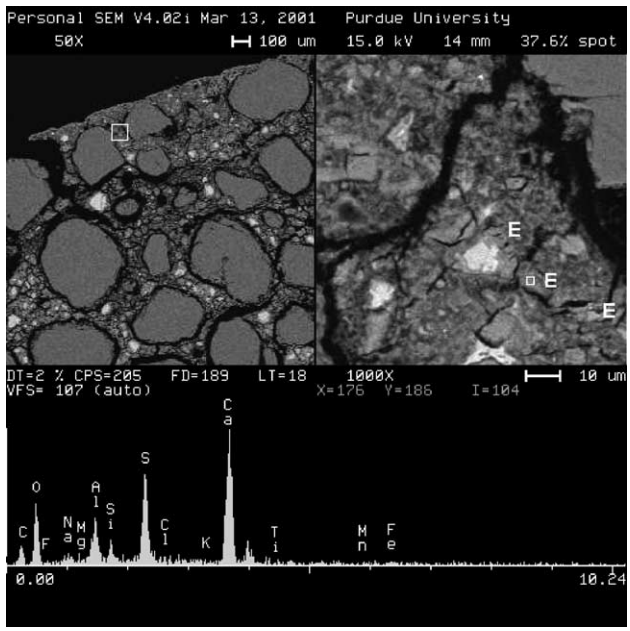

Fig. 9. PC mortar after 32 weeks of immersion in Na_2SO_4 solution, showing an abundant ettringite deposition (E) in the surface region.

low magnification images of Figs. 8–10. Gypsum deposits are not evident except in certain regions (Fig. 8). This could be a result of removal of disintegrated areas of the mortars that have been softened by the deposition of gypsum and are in direct contact with the solution. Indeed, some disintegrated pieces of soft mortar were observed on the floor of the container. Numerous deposits of ettringite were observed. Fig. 9 shows deposits of ettringite within the paste very close to the surface of the specimen. In fact, the white feature near the middle of the right hand image in Fig. 9 is a C_3A particle that is getting transformed to ettringite. Some ettringite deposits in and around the air voids are also observed (Figs. 10 and 11). The strong C peak shown in Fig. 10 is probably due to the epoxy that has embedded the highly cracked ettringite deposit. Thaumasite was present as small inclusions (mostly as an intimate mixture with ettringite) within the C–S–H as shown in Fig. 8.

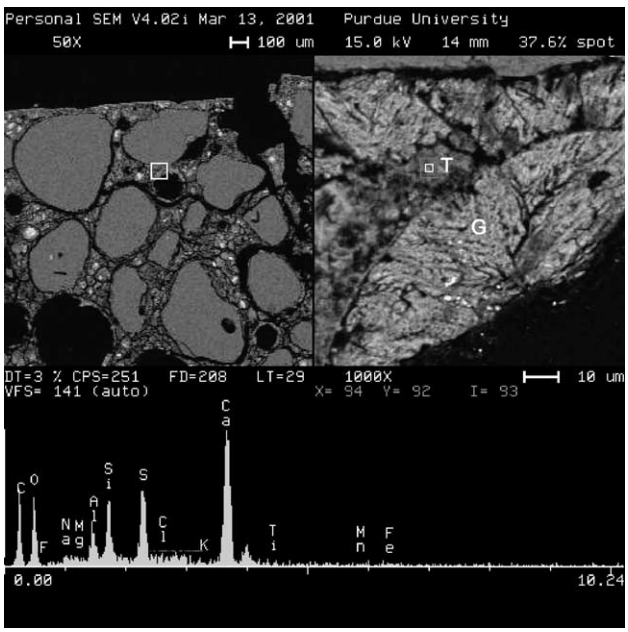

Fig. 8. PC mortar after 32 weeks of immersion in Na_2SO_4 solution, showing extensive gypsum deposition along with a small thaumasite (mixed with some ettringite) deposit in a severely cracked surface region.

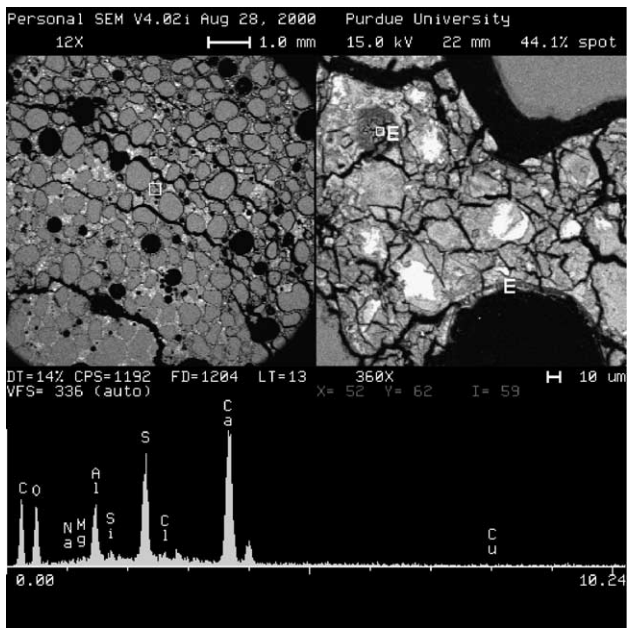

Fig. 10. PC mortar after 32 weeks of immersion in Na_2SO_4 solution, showing the deposition of ettringite (E) in a rim around an air void and in a cluster within the paste (upper left corner of the image on the right).

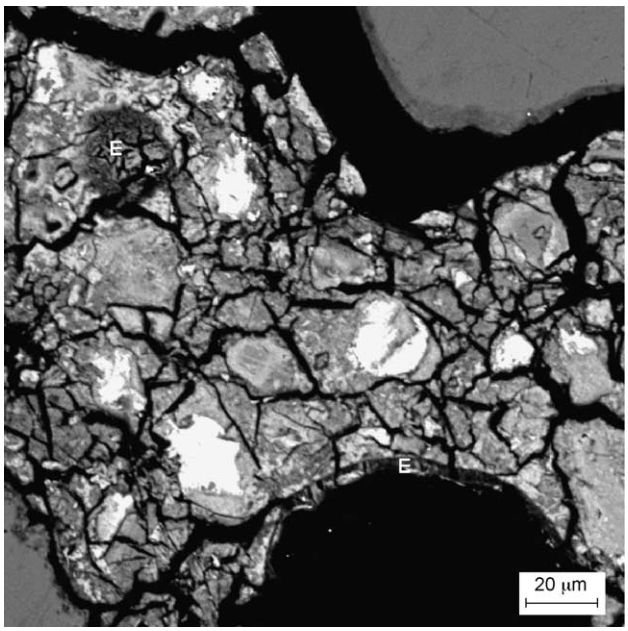

Fig. 11. Detailed view of the region in Fig. 10.

The micrographs for C_3S mortars in sodium sulfate solution after 41 weeks of immersion are presented in Figs. 12–14. Despite the long exposure period, the samples are relatively intact and the damage is mainly confined to a thin region near the surface. From the low magnification (left hand side) images in Figs. 12–14, the calcite layer on the surface is evident, along with a porous paste. The C–S–H in this region was found to be decalcified. However, no deposits of gypsum were detected up to a depth of about 300 μm from the surface. Beyond this depth, extensive gypsum deposition is observed lining air voids and also around aggregates. Some gypsum deposits were also seen within the paste. Thaumasite was detected to be present as small inclusions in the paste, especially in areas with a lot of gypsum deposition, as shown in Figs. 13 and 14.

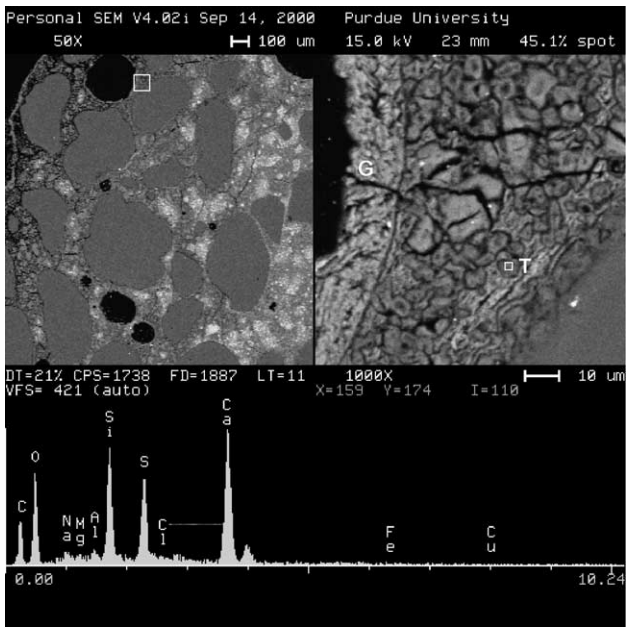

Fig. 13. C_3S mortar stored for 41 weeks in Na_2SO_4 solution, showing gypsum deposition in an air void, along with small inclusions of thaumasite (T) inside an area of extensively cracked and decalcified C–S–H; white deposits of gypsum can also be observed close to the thaumasite deposit.

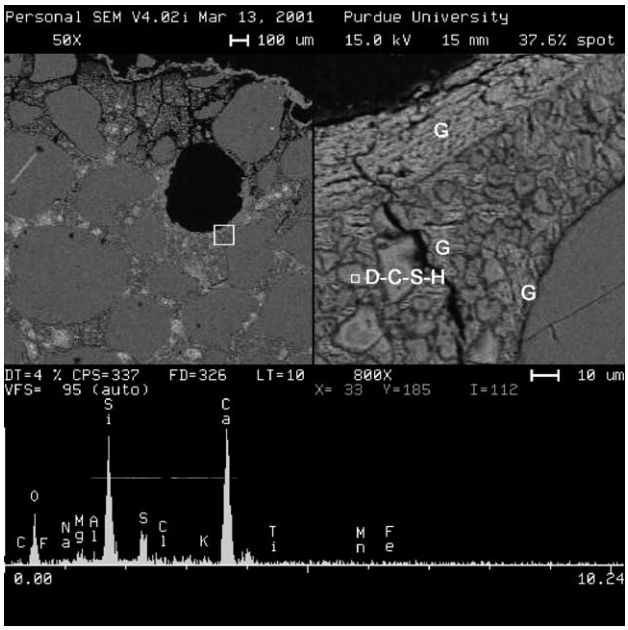

Fig. 12. C_3S mortar after 41 weeks of immersion in Na_2SO_4 solution, showing the deposition of gypsum (G) in an air void, in the paste, as well as around the aggregate; the C–S–H in this region was decalcified.

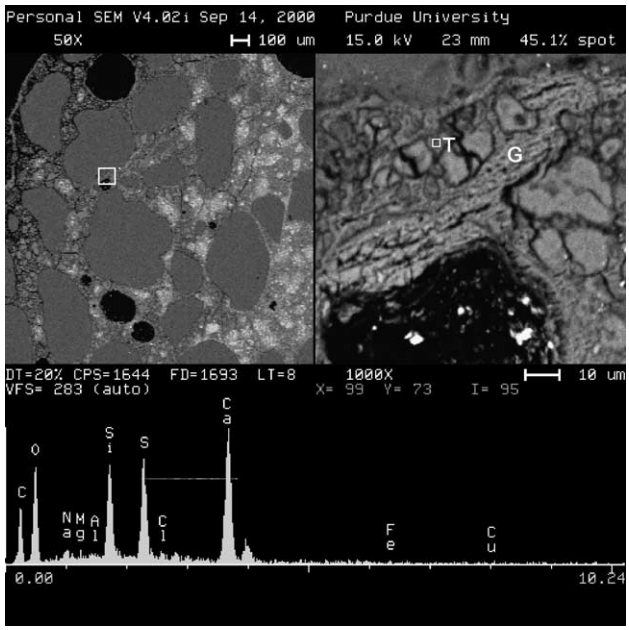

Fig. 14. Another small deposit of thaumasite near a region of abundant gypsum deposition in the C_3S mortar stored for 41 weeks in Na_2SO_4 solution.

4. Discussion

For the PC mortar, a considerable quantity of ettringite forms before any expansion of the mortar occurs. However, the sudden increase in expansion of the PC mortar is matched by the sudden jump in the quantity of gypsum, suggesting a possible expansive nature of gypsum. The quantity of ettringite also increases when the increase in expansion is registered. Thus, it is possible that the mortar system initially can accommodate the products formed by the sulfate attack reactions. When the quantity of attack products reaches a certain level, expansion occurs. By this philosophy, gypsum has to be contributing to the overall expansion. In the case of the PC mortar, the sudden increase in expansion occurs after the quantity of gypsum reaches almost 2% and the quantity of ettringite crosses 8%. For the C_3S mortar, expansion is registered after the quantity of gypsum reaches 2%. No ettringite forms in this case, so the expansion should be connected with the formation of gypsum.

Thaumasite was detected as small inclusions in both the systems (PC and C_3S). Thaumasite could not be quantified with the techniques used in this study, and the microstructural evidence showed extremely small amounts of thaumasite forming. Thus, it would be speculative to attribute any damage to the formation of thaumasite. The formation of thaumasite, despite absence of carbonate-bearing minerals, could be perhaps related to the carbonation of surface zones in both the PC and the C_3S mortars. Carbonation occurred in spite of continuous immersion in the solution, possibly because of the presence of dissolved CO_2 in the mix water as well as in the sulfate solution. Thaumasite formation was found to primarily occur in gypsum-rich areas when the C–S–H was carbonated. The evidence of thaumasite formation in a C_3A-free system shows that nucleation of thaumasite does not require the presence of ettringite, as is sometimes reported in the literature [10].

5. Conclusions

- Attack by sodium sulfate solution causes deterioration by forming gypsum and ettringite in the PC mortars, and only gypsum in the C_3S mortars. Results from expansion measurements and thermal analysis suggest that there is a possible link between the amount of gypsum and the measured expansion.
- Cracking and deterioration was higher in the PC mortar as compared to the C_3S mortar. This could be attributed to the abundant formation of ettringite in addition to gypsum in the PC mortar. The expansion of PC mortars was due to a combined effect of gypsum and ettringite formation, while the expansion of C_3S mortars was caused entirely by gypsum formation.
- Thaumasite formation in small inclusions within the paste was detected in both the PC and C_3S mortars. The formation of thaumasite does not have to be limited to low temperatures as evidenced by its occurrence in the samples cured at 25 °C. Carbonation of the surface zones in the mortars, possibly due to dissolved CO_2 in the solutions, caused the formation of thaumasite.

Acknowledgements

The Andrews Fellowship from Purdue University is gratefully acknowledged. Comments and suggestions from Prof. Sidney Diamond are also appreciated.

References

[1] S. Diamond, R.J. Lee, Microstructural alterations associated with sulfate attack in permeable concretes, in: J. Skalny, J. Marchand (Eds.), Material Science of Concrete-Sulfate Attack Mechanisms, American Ceramic Society, Westerville, OH, 1999, pp. 123–174.
[2] D. Bonen, M.D. Cohen, Magnesium sulfate attack on Portland cement paste: I. Microstructural analysis, Cem. Concr. Res. 22 (1992) 169–180.
[3] P.K. Mehta, D. Pirtz, M. Polivka, Properties of alite cements, Cem. Concr. Res. 9 (1979) 439–450.
[4] B. Tian, M.D. Cohen, Does gypsum formation during sulfate attack on concrete lead to expansion? Cem. Concr. Res. 30 (2000) 117–123.
[5] W.C. Hansen, Attack on Portland cement concrete by alkali soils and water—a critical review, Highw. Res. Rec. 113 (1966) 1–32.
[6] B. Mather, Discussion of "The process of sulfate attack on cement mortars", Adv. Cem. Based Mater. 5 (1996) 109–110.
[7] F.M. Lea, R.W. Nurse, Problems of crystal growth in building materials, Cryst. Growth: Discuss. Faraday Soc (5) (1949) 345–352.
[8] W.C. Hansen, Crystal growth as a source of expansion in Portland cement concrete, Proc. Am. Soc. Testing Mater. 63 (1963) 932–945.
[9] I. Biczok, Concrete Corrosion Concrete Protection, Chemical Publishing, NY, 1967.
[10] J. Bensted, Thaumasite-background and nature in deterioration of cements, mortars, and concretes, Cem. Concr. Compos. 21 (1999) 117–121.
[11] S.A. Hartshorn, J.H. Sharp, R.N. Swamy, Thaumasite formation in Portland–limestone cement pastes, Cem. Concr. Res. 29 (1999) 1331–1340.
[12] P.W. Brown, H.F.W. Taylor, The role of ettringite in external sulfate attack, in: J. Skalny, J. Marchand (Eds.), Material Science of Concrete-Sulfate Attack Mechanisms, American Ceramic Society, Westerville, OH, 1999, pp. 73–98.
[13] B. Erlin, D.C. Stark, Identification and occurrence of thaumasite in concrete, Highw. Res. Rec. 113 (1966) 108–113.